MALAYSIAN JOURNAL OF BIOCHEMISTRY & MOLECULAR BIOLOGY

The Official Publication of The Malaysian Society For Biochemistry & Molecular Biology (MSBMB)
http://mjbmb.org

PHYSICOCHEMICAL CHARACTERIZATION OF ASTAXANTHIN-Cu COMPLEXES

Sri Widyarti*, Bayu Dwi Prakoso, Shifaaun Najihah, Syahputra Wibowo, Zakia Hasna Fajar, Sofy Permana, Sutiman Bambang Sumitro*

Department of Biology, Faculty of Mathematics and Natural Sciences, Universitas Brawijaya, Malang 65145, East Java, Indonesia

*Corresponding Author: sutiman@ub.ac.id; swid@ub.ac.id

History
Received: 16th June 2023
Accepted: 5th September 2023

Keywords:

Astaxanthin; Cu; FTIR; SEM-EDS; XRD

Abstract

Astaxanthin (ASX) is a natural biological antioxidant acceptable as a dietary supplement and food colorant. ASX has unique molecular characteristics which form stable formations in the presence of metal ions. This study aims to analyze the astaxanthin-Cu complex using FTIR, SEM-EDS, and XRD. The synthesis of the complex carried on ratios 1:1, 1:2, and 2:1. Complex formation was determined using UV-Vis spectrum and then confirmed using FTIR. Although the profile spectrum UV-Vis has no differences between ratios, FTIR analysis showed an interaction between ASX with Cu. The SEM-EDS microstructure analysis showed that the ASX-Cu complex is a more regular form than astaxanthin alone. The analysis results based on X-ray diffraction showed that the crystal of astaxanthin, Cu, and each complex had different structures, asymmetric, and atomic arrangements. In conclusion, the ASX-Cu complex with a ratio of 1:1, 1:2, and 2:1 has been successfully made at the incubation time of 5 minutes at 20°C.

INTRODUCTION

Astaxanthin (3,3'-dihydroxy-â, â'-carotene-4,4'-dione) (ASX), a red carotenoid pigment that does not have pro-vitamin A activity, is a natural biological antioxidant found in various types of plant, algae, and biota of the sea [1]. ASX is considered the second most important carotenoid in the global market, with an income of around USD 288.7 million in 2017, and it is anticipated that it might be doubled by 2022 [2]. ASX has been approved for its safety application either as a dietary supplement or food colorant by the European Commission and The United States Food and Drug Administration (USFDA) in the food and beverages industries [3,4]. ASX has gained much interest in recent years as a human dietary supplement due to its antioxidative properties, which are ten times higher than β-carotene and 100-times higher than α-tocopherol [5,6]. Besides, ASX has multiple pharmacological benefits, such as antioxidant, anti-inflammatory, immunomodulatory, anticancer, and antidiabetic activities [7–11].

Free radicals and reactive oxygen species (ROS) will initiate cell oxidative damage. Both molecules have high reactivity, and their excessive production may damage the cellular machinery such as proteins, lipids, and DNA via radical chain reaction [12]. ASX can effectively protect fatty acids and biological membranes due to oxidative damage through its conjugated double bonds. The conjugated double bonds counteract the free radicals by donating its electron to produce a more stable output and terminate the free radical chain reactions [1]. Further, by reducing lipid peroxidation, ASX can reduce the cytotoxicity caused by glycated proteins [13,14]. During the reaction with O_2, energy is transferred from O_2 to the ASX molecule, turning it into an energy-rich triplet state. ASX in the triplet state can return to its basic state by releasing energy in heat, allowing the ASX molecule to accept oxygen. Interestingly, ASX demonstrated the best scavenging activity for peroxyl, and hydroxyl radicals than other carotenoids, with the scavenging activity of HO• reaching 66% and 17% greater than Trolox and quercetin, consecutively [15].

The unique molecular structure of ASX may enable the stable complexes formation with metal ions, such as Ca^{2+}, Cu^{2+}, Pb^{2+}, Zn^{2+}, Cd^{2+}, and Hg^{2+} [16,17]. Instead, the presence of metal cations induces the maximum absorption of ASX and gives a more red color [16]. In contrast, another study reported that ASX does not form chelate complexes with Cu^{2+} ions, but the electron transfer was still occurred [18]. Interestingly, ASX in a complex form with metals has shown better electron donor and electron acceptor properties than ASX alone [16]. A previous study reported that complexation ASX with copper chloride might improve and stabilize its antioxidant properties [19]. Despite the fact that transition metals such as Cu, Fe, and Zn are needed in small amounts in the diet as micronutrients, the complexes synthesis of ASX with metal ions may be expected to have a beneficial impact on the ASX action mechanism [20]. Subsequently, our current study is trying to analyze the physicochemical properties of ASX interact with Cu^{2+} as complexes that would add the new insight of ASX biofunction.

MATERIALS AND METHODS

Materials

Pure Astaxanthin was purchased from Sigma-Aldrich (SML0982 CAS No 472-61-7). Ethanol (absolute) and $CuSO_4.5H_2O$ were purchased from Merck. Deionized water was used in all experiments.

Methods

Preparation of Astaxanthin Stock Solution

A 0.167 mM Astaxanthin stock solution was prepared by weighing 10 mg of astaxanthin powder and transferred into 100 ml volumetric flask. After adding a small volume of ethanol, the volumetric flask was gently swirl until the astaxanthin powder dissolve. As the astaxanthin is completely dissolved, the volume was added up to 100 mL with ethanol and mixed thoroughly by inverting it several times [18]. The astaxanthin solution is kept in the aluminium foil wrapped bottle and ready to use.

Preparation of $CuSO_4.5H_2O$ Solution

A 0.04 M $CuSO_4.5H_2O$ solution was prepared by weighing 1.2 mg of $CuSO_4.5H_2O$ and dissolve in a small volume of distilled water. Once completely dissolved, the stock solution of CuSO4.5H2O was dilute with distilled water to final volume of 120 ml and mixed thoroughly by gentle swirling.

Preparation of Astaxanthin-Cu Complex Solution

The astaxanthin stock solution and $CuSO_4.5H_2O$ stock solution were diluted to concentrations of 0.04 mM and 0.02 mM. The complex was made in ratio 1:1, 1:2, and 2:1. The $CuSO_4.5H_2O$ solution was mixed into the astaxanthin solution while stirring gently for 5 minutes at a temperature 20°C. The Astaxanthin-Cu complex solution is now ready to analysis.

Spectrum UV-Vis Analysis

Complex formation based on UV-Vis spectrum profile is determined using Genesys 10 UV at a wavelength of 200-800 nm equipped with 1.0 cm quartz cells at room temperature.

Fourier-Transform Infrared (FTIR) Spectroscopy Analysis

All samples were lyophilized using a freeze dryer. The lyophilized sample (1 mg) and KBr were homogenized into a powder and then compacted on a disc. Samples were analyzed on an FTIR spectrometer (Shimadzu 8400S) in the range of 400–4000 cm^{-1} at room temperature. Pure KBr disks were used for zeroing.

SEM-EDS Analysis

Samples in the form of freeze-dried powder were carried out on Al 12 mm pin stub with a carbon tape base, then air-dried in a chamber containing silica gel. The instrument used was SEM (FEI Quanta FEG 650) FE-SEM type, equipped with INCAx-act_80952 X-act Oxford Instrument detector and AztecOne EDS software. The EDS settings are performed at low vacuum, 10 kV, pressure 80 Pa, spot 4, dwell t 1 us, WD 10 mm, SEM Image detector LFD (SE image).

X-ray Diffractometry (XRD) Analysis

The freeze-dried powders of samples were packed tightly in a rectangular aluminum cell. The samples were exposed to the X-ray beam from an X-ray generator running at 36 kV and 20 mA. The scanning regions of the diffraction angle, 2θ, were 5–60°. Radiation was detected with a proportional detector.

RESULTS AND DISCUSSION

Spectrum UV Profile

The UV-Vis spectrum profile formed does not follow the astaxanthin but the Cu complex profile (Figure 1). However, the ASX-Cu profile has a higher absorbency intensity than the Cu ion peak. In the visible spectrum, the ASX-Cu complex has a higher absorbance than Cu ions and tends to increase. Based on the evaluation of the absorbance value of the complex in the UV-Vis spectrum, the complex is formed at a temperature of 20ºC for 5 minutes, which applies to a ratio of 1:1, 1:2, and 2:1. However, the spectrum UV profile has no differences between ratios. The previous study reported that the peak of free ASX was observed at 486 nm [21]. The peak shift between ASX only and ASX complexes was due to a hypsochromic or blue shift, which occurred when the maximum absorbance moved towards a shorter wavelength. The $CuCl_2$ absorption might interfere with the formation of the H-type aggregate, which indicates a tight association in hypsochromic shift [17].

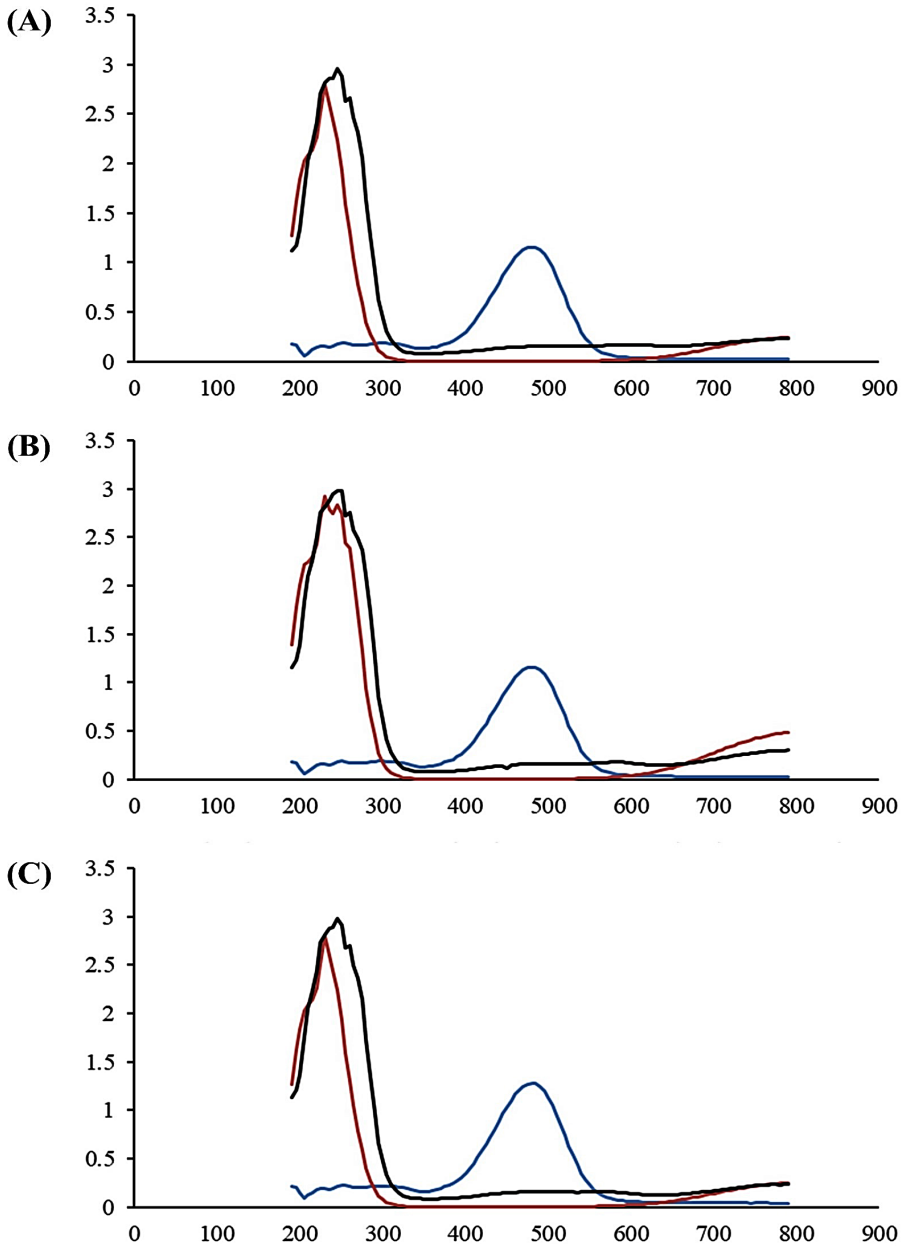

Figure 1. UV Profile of ASX-Cu complexes. (A) ASX:Cu 1:1. (B) ASX:Cu 1:2. (C) ASX:Cu 2:1. The line indicated: blue = the absorbance of ASX, red = the absorbance of Cu, and black = The absorbance of complex.

Our present result demonstrated that ASX alone followed J-type aggregates. These molecular excitation models described that the individual monomers dipole of ASX was aligned end to end or head to tail arrangements [22]. Surprisingly, as we stated before, the ASX-Cu complexes were followed the Cu absorbance pattern (Figure 1). The result can suggest that the Cu molecules were attached to the ASX molecule's head. Besides, a previous study demonstrated that the synthesis of ASX with $CuCl_2$ at room temperature might attach these two molecules to form complexes through the carbonyl and hydroxyl groups interaction [19]. The appearance of a shoulder at 600 nm in ASX complexes (Figure 1A-C) might be from the electron transfer from ASX to the metal ion, leading to the formation of ASX radical cation, which has high stability [18].

FTIR Analysis

The ASX-Cu complex was characterized based on the FTIR profile to investigate the formed complexes between ASX with Cu for further observation. ASX is a large polyene chain terminated with singly unsaturated chiral rings. A reduction in the intensity at a wave number of 1664-1552 cm^{-1} indicates a change in the group and the formation of bonds with Cu, which can be seen as vibrations at a wavenumber of 1000-500 cm^{-1}. Increasing absorption of 1000-500 cm^{-1} in the three complexes compared to ASX alone indicates the presence of metallic bonds with donor atoms of ASX (Figure 2).

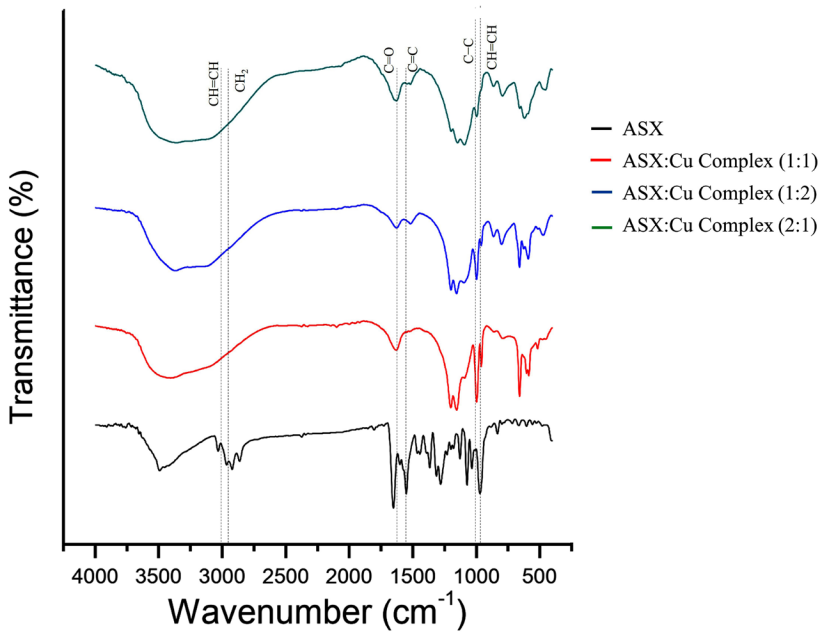

Figure 2. FTIR profile of ASX-Cu Complexes.

The typical peaks of ASX at 1651, 1552, 976, and 960 cm^{-1} were assigned to the C–O, C=C, and C–H stretching vibration peaks of the molecular skeleton, respectively [23]. Figure 2 exhibits the FTIR spectra of astaxanthin, astaxanthin-Cu 1:1, 1:2, 2:1. The ASX characteristics revealed absorption bands at 3010 cm^{-1} for the trans −CH=CH, 2925 and 2855 cm^{-1} for asymmetric and symmetric stretching of the CH_2, 1650 or 1654 cm^{-1}, which may reflect the shift of C=O mainly to the presence of hydrogen bond in dimer form, 1552 cm^{-1} is assigned for C=C stretching vibration in the aromatic ring, 1280 and 1074 cm^{-1} is attributable to C-O stretching vibrations, and 972 cm^{-1} for the trans conjugated alkene −CH=CH− [24–26]. A reduction in the intensity at a wave number of 1664-1552 cm^{-1} indicates a change in the group and the formation of bonds with Cu, which can be seen as vibrations at a wavenumber of 1000-500 cm^{-1}. Increasing absorption of 1000-500 cm^{-1} in the three complexes compared to ASX alone indicates the presence of metallic bonds with donor atoms of ASX. A previous study demonstrated that the increased charge of metal ions was due to the weakening of C−O bonds, which further form an oxidation state during the transition [27]. ASX can form chelate complexes with metal ions such as Cu because of the presence of hydroxyl (–OH) and keto (C=O) groups at position(s) C3(C3') and C4(C4') symmetrically on both cyclohexene rings [28]. A previous study demonstrated that the interaction of Cu with ASX was detected in the FTIR by a peak at the wave number 600-400 cm^{-1}, which indicated a Cu-O group bond [17].

Microstructure Analysis (SEM-EDS)

SEM-EDS analysis is a non-destructive analysis technique that uses electron radiation to produce a typical x-ray emission for each element. Scanning electron microscopy micrograph showed differences in surface microstructure in astaxanthin-Cu. Pure astaxanthin was an irregularly lumpy crystal. After synthesizing, the astaxanthin-Cu complex showed a regularly tubular form. The size of the complex reduces on ratios 1:2 and 2:1. The EDS spectrum of the ASX-Cu complex presented peaks corresponding to carbon, oxygen, and Cu elements that confirmed the elemental composition of the complex. EDS shows the percentage range of the elements in the complex astaxanthin-Cu, visualized in the adequate voltage range (keV), counted in seconds per electron-volt (cps/eV). The presence and distribution of Cu are found in the astaxanthin-Cu complex, whereas a single ASX is not detected for the presence of Cu (Figure 3).

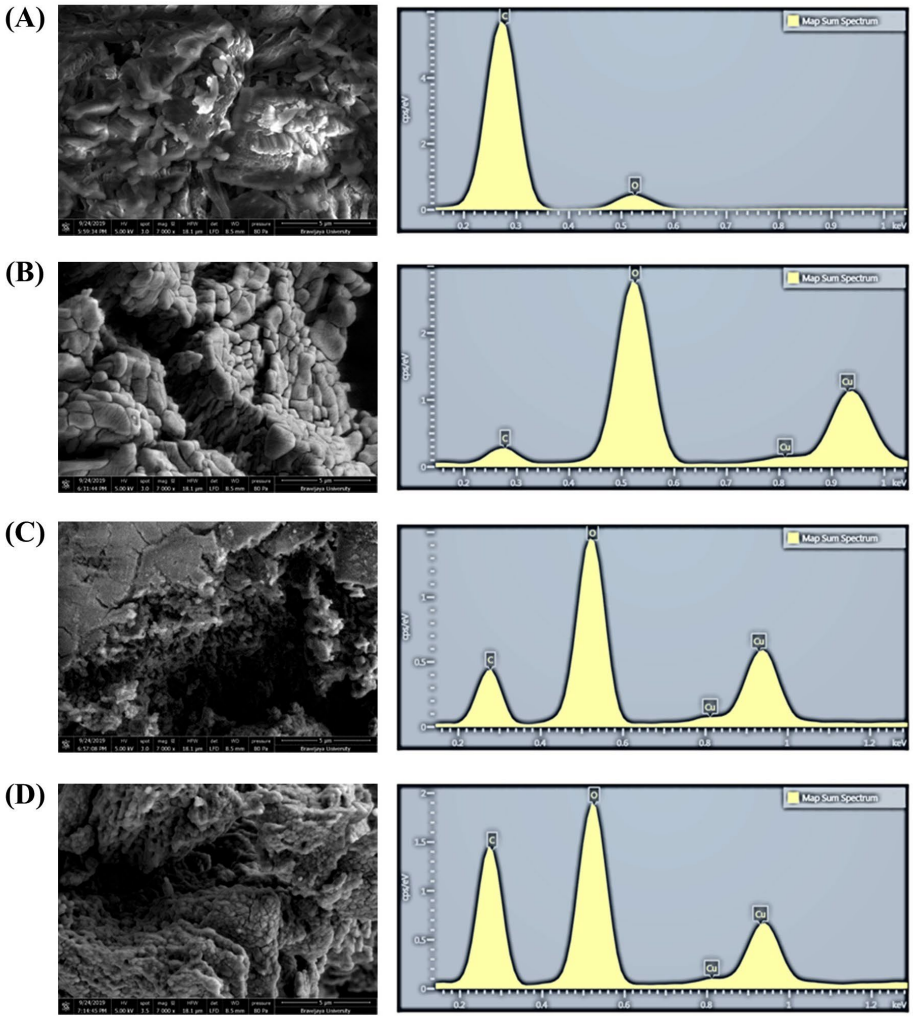

Figure 3. Surface Microstructure and EDS Results of ASX-Cu Complexes. (A) ASX only; (B) ASX:Cu 1:1. (C) ASX:Cu 1:2. (D) ASX:Cu 2:1.

Table 1. The percentage range of the elements

Element	Pure Astaxanthin		Astaxanthin: Cu 1:1		Astaxanthin: Cu 1:2		Astaxanthin: Cu 2:1	
	Weight %	Weight % Sigma	Weight %	Weight % Sigma	Weight %	Weight % Sigma	Weight %	Weight % Sigma
C	**83.10**	0.96	38.08	0.93	20.08	1.30	35.40	1.07
O	16.90	0.96	**52.80**	1.10	**49.55**	1.43	**44.14**	1.08
Cu	-	-	38.08	1.10	29.77	1.42	20.45	1.00

Pure astaxanthin has a strong peak at 0,28 keV confirm the presence of the C element, while a low peak at 0,523 keV confirms the presence of the O element. Otherwise, complex ASX-Cu has a strong peak at the O element and a low peak at the C element. Most of these peaks are X-rays given off as electrons return to the K electron shell. Cu has a strong peak at 0,94 keV and a low peak at 0,80 keV on pure ASX and complex ASX-Cu. Most of these peaks are X-rays given off as electrons return to the L electron shell. The interaction of Cu on astaxanthin causes decreasing the cps/eV value of the C element but increasing one of the O elements. Based on its molecular structure, astaxanthin has unique properties.

Results of XRD

The crystalline status of ASX, Cu, and ASX-Cu was determined based on X-Ray diffraction analysis. The diffractograms results revealed that ASX has several sharp peaks at 2θ 10-300° while the Cu peak is at 2θ 20-800°. After forming the complex, the ASX-Cu peak lies at 2θ 20-800.

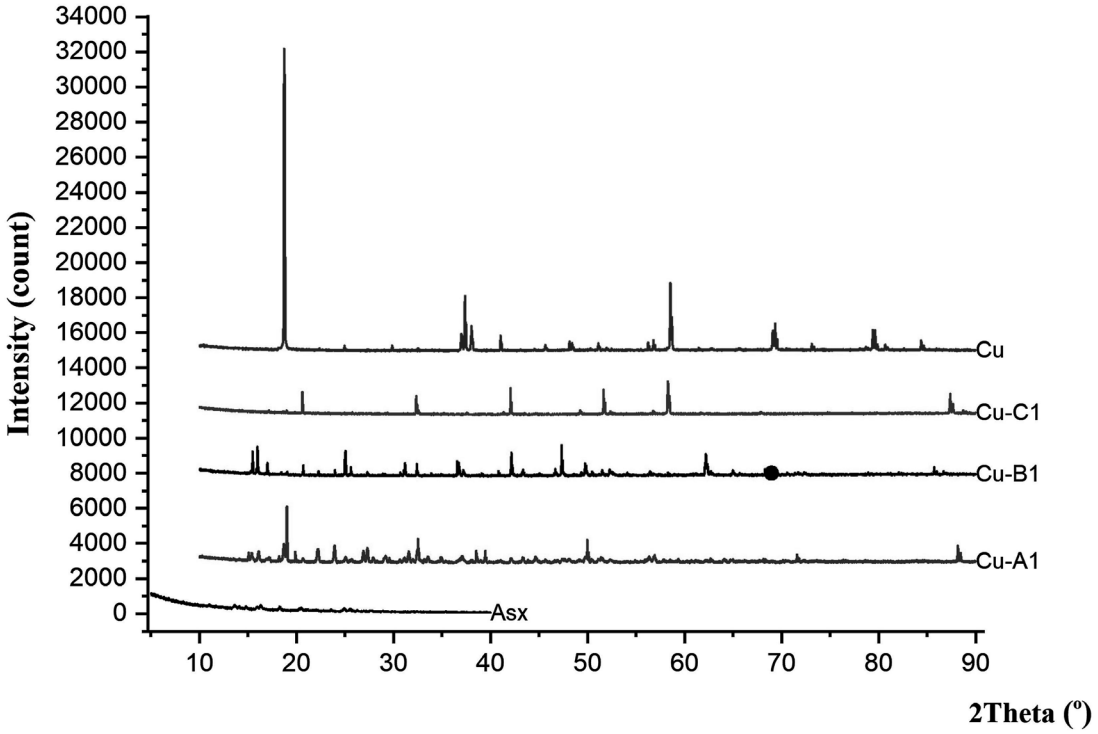

Figure 4. Diffractograms of Astaxanthin-Cu complex. (A) ASX only; (B) ASX:Cu 1:1. (C) ASX:Cu 1:2. (D) ASX:Cu 2:1.

Peak XRD ASX resembles that presented by Pan et al. [25]. This suggests that ASX mainly exists in a crystalline form. Intriguingly, our present studies depicted that Cu has the most intense peaks compared to the ASX peaks pattern. In contrast, these intensity peaks were reduced in Cu-ASX A1-C1 (Figure 4). This suggests that Cu has shifted from a crystalline to an amorphous state in the complex [29]. The amorphous state exhibit an advantage through the higher solubility of the complex formed than the unprocessed materials [30].

Further, it is observed that the results of the astaxanthin-Cu diffractogram are more similar to the Cu diffractogram than ASX. This is in line with the UV spectrum profile of ASX-Cu, which is closer to the Cu spectrum profile than ASX. The peak of the ASX-Cu diffractogram at a location greater than 300 shows a change in the crystalline structure of ASX after interacting with Cu. The difference in the position of the peak diffractogram on ASX, Cu and the complex shows that there are differences in crystal structure. The number of diffractogram peaks in ASX, Cu or the complex indicates that the structure of crystalline formed is not symmetrical. The difference in the intensity of the diffractogram peaks in ASX, Cu and the complex shows the different arrangement of atoms in the crystal. In conclusion, the results showed up to now are that the ASX-Cu complex has been successfully made with a ratio of 1:1, 1:2, and 2:1 at the incubation time of 5 minutes at 20°C. Further research is required to examine the ASX-Cu complexes and their pharmacological properties for suitable nutraceuticals in the future.

ACKNOWLEDGEMENTS

This research was funded by Direktorat Riset dan Pengabdian Masyarakat Pengembangan Kementerian Riset, Teknologi, dan Direktorat Jenderal Penguatan Riset dan

Pendidikan Tinggi with contract number 055/SP2FVLT/DRPM/2019.

CONFLICT OF INTEREST

The authors declare that there is no conflict of interests regarding the publication of this manuscript.

REFERENCES

1. Ambati R.R., Phang S.M., Ravi S., Aswathanarayana, R. (2014). Astaxanthin: sources, extraction, stability, biological activities and its commercial applications--a review. *Mar Drugs* **12**: 128–152.
2. McWilliams A. (2018). The Global Market for Carotenoids, Wellesley, MA, USA, BCC Research.
3. Pashkow F.J., Watumull D.G., Campbell C.L. (2008). Astaxanthin: A Novel Potential Treatment for Oxidative Stress and Inflammation in Cardiovascular Disease. *The American Journal of Cardiology* **101**: S58–S68.
4. Solymosi K., Latruffe N., Morant-Manceau A., Schoefs B. (2015). Food colour additives of natural origin, *Colour Additives for Foods and Beverages*, Elsevier, 3–34.
5. Miki W. (1991). Biological functions and activities of animal carotenoids. *Pure and Applied Chemistry* **63**: 141–146.
6. Cuellar-Bermudez S.P., Aguilar-Hernandez I., Cardenas-Chavez D.L., Ornelas-Soto N., Romero-Ogawa, M.A., Parra-Saldivar R. (2015). Extraction and purification of high-value metabolites from microalgae: essential lipids, astaxanthin and phycobiliproteins. *Microbial Biotechnology* **8**: 190–209.
7. Lin K-H., Lin K-C., Lu W-J., Thomas P.A., Jayakumar T., Sheu J.R. (2015). Astaxanthin, a Carotenoid, Stimulates Immune Responses by Enhancing IFN-γ and IL-2 Secretion in Primary Cultured Lymphocytes in Vitro and ex Vivo. *IJMS* **17**: 44.
8. Farruggia C, Kim M-B, Bae M, Lee Y., Pham T.X., Yang Y., Han M.J., Park Y.K., Lee J.Y. (2018). Astaxanthin exerts anti-inflammatory and antioxidant effects in macrophages in NRF2-dependent and independent manners. *The Journal of Nutritional Biochemistry* **62**: 202–209.
9. Hormozi M., Ghoreishi S., Baharvand P. (2019). Astaxanthin induces apoptosis and increases activity of antioxidant enzymes in LS-180 cells. *Artificial Cells, Nanomedicine, and Biotechnology* **47**: 891–895.
10. Zhuge F., Ni Y., Wan C., Liu F., Fu Z. (2021). Anti-diabetic effects of astaxanthin on an STZ-induced diabetic model in rats. *Endocr J* **68**: 451–459.
11. Fouad M.A., Sayed-Ahmed M.M., Huwait E.A., Hafez H.F., Osman A.M. (2021) Epigenetic immunomodulatory effect of eugenol and astaxanthin on doxorubicin cytotoxicity in hormonal positive breast Cancer cells. *BMC Pharmacol Toxicol* **22**: 8.
12. Blokhina O. (2003) Antioxidants, Oxidative Damage and Oxygen Deprivation Stress: a Review. *Annals of Botany* **91**: 179–194.
13. Nishigaki I., Rajendran P., Venugopal R., Ekambaram G., Sakthisekaran D., Nishigaki Y. (2010). Cytoprotective role of astaxanthin against glycated protein/iron chelate-induced toxicity in human umbilical vein endothelial cells. *Phytother Res* **24**: 54–59.
14. Park C.H., Xu F.H., Roh S-S., Song Y.K., Uebaba K., Noh J.S., Yokozawa T. (2015). Astaxanthin and Corni Fructus Protect Against Diabetes-Induced Oxidative Stress, Inflammation, and Advanced Glycation End Product in Livers of Streptozotocin-Induced Diabetic Rats. *Journal of Medicinal Food* **18**: 337–344.
15. Rodrigues E., Mariutti L.R.B., Mercadante A.Z. Mariutti L., Mercadante A.Z. (2012). Scavenging Capacity of Marine Carotenoids against Reactive Oxygen and Nitrogen Species in a Membrane-Mimicking System. *Marine Drugs* **10**: 1784–1798.
16. Hernández-Marin E., Barbosa A., Martínez A. (2012). The Metal Cation Chelating Capacity of Astaxanthin. Does This Have Any Influence on Antiradical Activity? *Molecules* **17**: 1039–1054.
17. Wibowo S., Prakoso B.D., Najihah S, Fajar Z.H., Widyarti S., Sabarudin A., Soeatmadji W.D., Sumitro S.B. (2021). Synthesis and Characterization of Astaxanthin Metal Ions (Cu2+ and Zn2+) Complex. *RJC* **14**: 877–886.
18. Polyakov N.E., Focsan A.L., Bowman M.K., Kispert L.D. (2010). Free Radical Formation in Novel Carotenoid Metal Ion Complexes of Astaxanthin. *J Phys Chem B* **114**: 16968–16977.
19. Shuaith N, Farrel G. (2015). Synthesis and characterisation of novel astaxanthin metal complexes. Thesis. Letterkenny Institute of Technology: Ireland
20. Wibowo S., Widyarti S., Sabarudin A., Soeatmadji D.W., Sumitro S.B. (2021). DFT and molecular dynamics studies of astaxanthin-metal ions ($Cu2^{+}$ and Zn^{2+}) complex to prevent glycated human serum albumin from possible unfolding. *Heliyon* **7**: e06548.
21. Wibowo S, Costa J, Baratto MC, et al. (2022) Quantification and Improvement of the Dynamics of Human Serum Albumin and Glycated Human Serum Albumin with Astaxanthin/Astaxanthin-Metal Ion Complexes: Physico-Chemical and Computational Approaches. IJMS 23: 4771.
22. Johal M., Johnson L. (2017). Understanding Nanomaterials, Second Edition, Boca Raton, CRC Press.
23. Dai M., Li C., Yang Z., Sui Z., Li J., Dong P., Liang X. (2020). The Astaxanthin Aggregation Pattern Greatly Influences Its Antioxidant Activity: A Comparative Study in Caco-2 Cells. *Antioxidants* **9**: 126.
24. Liu J., Huang Q. (2016). Screening of Astaxanthin-Hyperproducing *Haematococcus pluvialis* Using Fourier Transform Infrared (FT-IR) and Raman Microspectroscopy. *Appl Spectrosc* **70**: 1639–1648.
25. Pan L., Zhang S., Gu K., Zhang N. (2018). Preparation of astaxanthin-loaded liposomes: characterization, storage stability and antioxidant activity. *CyTA - Journal of Food* **16**: 607–618.
26. Liu J, Chen X, Yang X, Chen J., Qi Z. (2019). Astaxanthin accumulation in Haematococcus pluvialis observed through Fourier-transform infrared microspectroscopy imaging. *Journal of Molecular Structure* **1182**: 119–122.
27. Focsan A., Polyakov N., Kispert L. (2017). Photo Protection of Haematococcus pluvialis Algae by Astaxanthin: Unique Properties of Astaxanthin Deduced by EPR, Optical and Electrochemical Studies. *Antioxidants* **6**: 80.
28. Debus RJ (2015) FTIR studies of metal ligands, networks of hydrogen bonds, and water molecules near the active site Mn4CaO5 cluster in Photosystem II. *Biochimica et Biophysica Acta (BBA) - Bioenergetics* **1847**: 19–34.
29. Sun S-B., Liu P., Shao F-M., Miao Q.L. (2015) Formulation and evaluation of PLGA nanoparticles loaded capecitabine for prostate cancer. *Int J Clin Exp Med* 8: 19670–19681.
30. Jog R., Burgess D.J. (2017) Pharmaceutical Amorphous Nanoparticles. *Journal of Pharmaceutical Sciences* **106**: 39–65.